nature neuroscience



# Protocadherin Celsr3 is crucial in axonal tract development

Fadel Tissir[1,3], Isabelle Bar[2,3], Yves Jossin[1] & Andre M Goffinet[1]

**In the embryonic CNS, the development of axonal tracts is required for the formation of connections and is regulated by multiple genetic and microenvironmental factors. Here we show that mice with inactivation of *Celsr3*, an ortholog of *Drosophila melanogaster* flamingo (*fmi*; also known as starry night, *stan*) that encodes a seven-pass protocadherin, have marked, selective anomalies of several major axonal fascicles, implicating protocadherins in axonal development in the mammalian CNS for the first time. In flies, *fmi* controls planar cell polarity (PCP) in a frizzled-dependent but wingless-independent manner. The neural phenotype in *Celsr3* mutant mice is similar to that caused by inactivation of *Fzd3*, a member of the frizzled family. *Celsr3* and *Fzd3* are expressed together during brain development and may act in synergy. Thus, a genetic pathway analogous to the one that controls PCP is key in the development of the axonal blueprint.**

The protocadherin genes *Celsr1–Celsr3* (refs. 1,2) are mammalian orthologs of Drosophila flamingo (*fmi*)[3,4] that are expressed in the developing mouse brain with complementary patterns[5–8]. They are predicted to encode proteins larger than 3,000 amino acids with N-terminal cadherin repeats, a G protein–coupled receptor proteolysis site (GPS), seven transmembrane segments (7TM) and an intracellular C-terminus. The amino acid sequences of Celsr1–Celsr3 are more than 50% identical in extracellular and transmembrane regions, but their cytoplasmic tails differ, suggesting that they mediate distinct signaling cascades. Whereas *Celsr1* mRNA expression is confined to zones of neural precursor proliferation, *Celsr2* mRNA is detected in both germinative and postmitotic fields and remains high in the adult. In contrast, *Celsr3* mRNA levels are higher in postmitotic neurons and are downregulated at the end of maturation[6–8]. In Drosophila, *fmi* null mutations are embryonically lethal as a result of defective longitudinal tracts in the CNS[3,4]. Viable flies generated by hypomorphic alleles or CNS-specific rescue have anomalies in the disposition of hairs on the wings and body and in ommatidial rotation in the eye. These defects in planar cell polarity (PCP) are dependent on frizzled but not wingless, placing *fmi* along with frizzled (*fz*), dishevelled (*dsh*), van gogh (*vang*; also known as strabismus (*stbm*)) and prickle (*pk*) among the so-called 'core PCP genes'[3,4,9–11]. In mice, inactivation of orthologs of PCP genes such as *Celsr1* (ref. 12) and *Ltap* (also known as *Vangl2* (van gogh–like 2), mutated in loop-tail mice)[13,14], or double mutations of *Dvl1* and *Dvl2* (dishevelled 1 and dishevelled 2; ref. 15), all perturb neural tube closure, showing that in mammals, a genetic pathway related to PCP is involved in this process.

Here we used gene inactivation in mice to show that the protocadherin gene *Celsr3* is critical for the development of several major axonal bundles in the CNS. In contrast, *Celsr3* does not affect prenatal dendritic development and cortical maturation. The neural phenotype in *Celsr3* mutant mice is similar to that generated by inactivation of *Fzd3*, a member of the frizzled family[16], and both genes are expressed in the developing brain. These results identify a genetic pathway, probably analogous to those that regulate PCP and neural tube closure, that is essential in fiber tract formation.

## RESULTS

### *Celsr3* gene inactivation

We designed a targeting construct to delete exons 19–27 of the mouse *Celsr3* gene, and we generated a heterozygous mutant embryonic stem cell line by homologous recombination (**Fig. 1a** and **Supplementary Note**, **Supplementary Table 1** and **Supplementary Fig. 1** online). Chimeric mice, produced by aggregation with CD1 morulae, were crossed to CD1 mice, and the mutation was kept on CD1 as well as backcrossed to C57Bl/6 mice. A mutant mRNA was present in mutant brains at a concentration (estimated by real time RT-PCR) two- to fourfold lower than in normal brains. RT-PCR sequencing confirmed deletion of exons 19–27. A cryptic acceptor site was used in modified intron 27, resulting in an 87-nucleotide 5′ extension of exon 28. The mutant mRNA encodes a predicted protein of 2,262 amino acids that is identical to Celsr3 up to residue 2,248 but lacks the GPS, the 7TM and the C-terminal cytoplasmic sequences. If present, this protein would be secreted or retained in the cell but not targeted to the plasma membrane[17] and unable to signal. The targeted allele was therefore presumed to be null.

### *Celsr3* mutant mice die neonatally from ventilation failure

Homozygous *Celsr3* mutant mice were born in mendelian proportions but died a few hours after birth. The phenotype was not modified by

[1]Developmental Neurobiology Unit, University of Louvain Medical School, 73, avenue Mounier, Box DENE7382, B-1200 Brussels, Belgium. [2]Molecular Physiology Research Unit, University of Namur Medical School, 61, rue de Bruxelles, B5000 Namur, Belgium. [3]These authors contributed equally to this work. Correspondence should be addressed to A.M.G. (andre.goffinet@dene.ucl.ac.be).

Published online 20 March 2005; doi:10.1038/nn1428

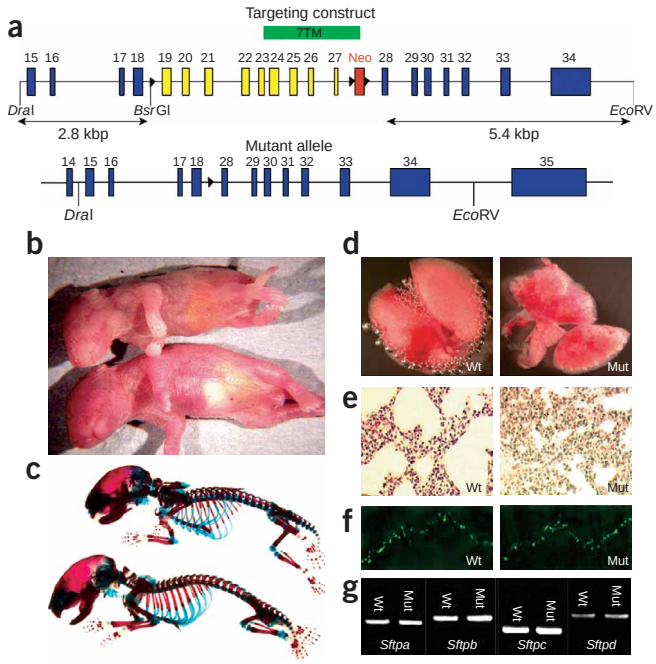


**Figure 1** Targeting strategy and phenotype of *Celsr3* mutant mice. (**a**) A 12-kbp *Dra*I-*Eco*V genomic fragment was cloned into pBluescript. A *lox*P site was inserted in intron 19 in a *Bsr*GI site, and a floxed *neo* cassette in intron 27 (in a *Sna*BI site). A mutant allele with deletion of exons 19–27 (yellow) was created by homologous recombination followed by Cre-mediated deletion in E14 embryonic stem cells. Chimeric mice were produced by aggregation to CD1 morulae. 7TM, seven transmembrane domains. (**b**) Comparison of a *Celsr3* mutant (top) and normal (bottom) neonate. Note cyanosis and absence of milk in the stomach of the mutant. (**c**) Skeletons of the mutant (top) and normal neonates, stained with alcian blue and alizarin red. (**d**) After immersion in buffer, bubbles form rapidly around normal (Wt: wild-type) but not mutant (Mut) lungs. (**e**) Histological preparations of normal and mutant lungs. Hematoxylin-eosin stain. (**f**) Ramifications of the phrenic nerves, shown in whole-mount preparations of the normal and mutant diaphragm, stained with anti-neurofilament antibodies. (**g**) Expression of the surfactant protein genes *Sftpa1*, *Sftpb*, *Sftpc* and *Sftpd*, detected by RT-PCR in normal and mutant lung RNA.

backcrossing to C57Bl/6 (four backcrosses) and CD1 (six backcrosses) mice. Newborn mutant mice showed poorly coordinated movements and progressive cyanosis. The body (**Fig. 1b**) and skeleton (**Fig. 1c**) were normal. Gross examination showed air dilatation of the stomach and upper duodenum and poorly inflated lungs, albeit with a normal lobular pattern. After immersion of lungs in buffer, bubbles formed rapidly around the normal but not the mutant tissue, confirming the reduction of air content in the mutant lungs (**Fig. 1d**). Despite the reduced alveolar space, all components of lung tissue were normal (**Fig. 1e**). No *Celsr3* mRNA was detected in normal embryonic lungs by *in situ* hybridization. Anti-neurofilament immunohistochemistry showed normal terminal ramifications of the phrenic nerves in mutant and control diaphragms (**Fig. 1f**). Using RT-PCR, we obtained a comparable amplification of the four surfactant protein genes, *Sftpa1*, *Sftpb*, *Sftpc* and *Sftpd* (oligonucleotide sequences in **Supplementary Table 2** online) with normal and mutant lung cDNA, indicating that lung hypoinflation was not related to a decrease in surfactant-producing cells (**Fig. 1g**). A histopathological examination of somatic organs from embryonic day 12.5 (E12.5) to birth did not show any anomaly. The heart and heart outflow tract were normal. Together with the neuropathological anomalies described below, these observations suggested that *Celsr3* mutant mice die of central ventilation failure.

### *Celsr3* inactivation affects major axonal tracts

CNS development was studied using hematoxylin-eosin and anti-neurofilament staining. Staining of whole-mount preparations of mutant and control embryos aged E10.5 and E11.5 showed that peripheral neural structures were normal in mutant embryos. We did not observe any anomalies in peripheral nerves, dorsal root ganglia and autonomic ganglia in sections from E12.5 to P0, but we did observe a marked malformation in the forebrain. Already detectable at E14.5 (**Fig. 2a**,**b**), it was the most evident at P0 (**Fig. 2c–h**). In mutant animals, the cortical wall was abnormally thin, mostly because of hypotrophy of the intermediate zone. The anterior commissure and the internal capsule were absent, and fiber bundles did not cross the striatum. The pallidum had a rounded shape, and the globular striatum protruded excessively into a moderately enlarged ventricle. The corpus callosum, the hippocampal formation and commissure, the hypothalamic region and epithalamic structures were normal. Because of

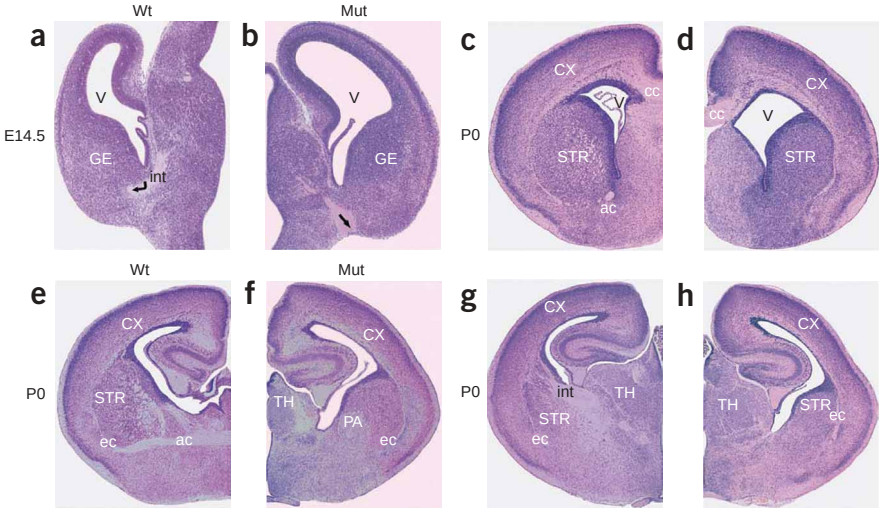


**Figure 2** Structure of the mutant and normal brain (paraffin sections, hematoxylin-eosin stain). (**a**,**b**) Comparison of the normal (Wt, **a**) and mutant (Mut, **b**) embryonic brain at E14.5. In the mutant brain, the internal capsule (curved arrow in **a**) is replaced by an aberrant bundle (arrow in **b**). (**c**–**h**) Rostrocaudal sections at P0. The anterior commissure and internal capsule are visible in the normal (**c**,**e**,**g**) but not in the mutant brain (**d**,**f**,**h**). The mutant striatum and pallidum are abnormal. CX, cortex; GE, ganglionic eminence; PA, pallidum; STR, striatum; TH, thalamus; ac, anterior commissure; int, internal capsule; ec, external capsule; V, ventricle.

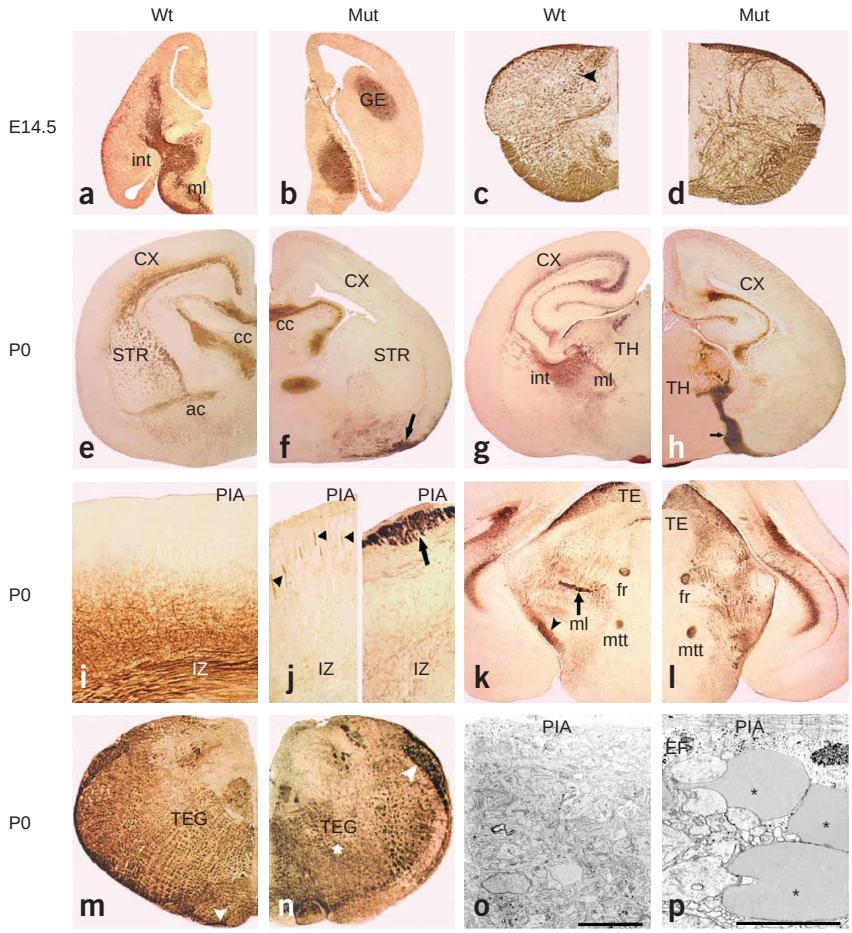


**Figure 3** *Celsr3* inactivation affects fiber tract development (paraffin sections, immunohistochemistry with 2H3 antineurofilament antibody). (**a**–**d**) Sections in forebrain (**a**,**b**) and spinal cord (**c**,**d**) at E14.5. Normal internal capsule and medial lemniscus (Wt, **a**) are absent in mutant brain (Mut, **b**). In the spinal cord, more fibers are present in the normal (arrowhead in **c**) than in the mutant (**d**) animal. (**e**–**h**) Sections in P0 forebrain. Labeled bundles cross the normal (**e**) but not the mutant (**f**) striatum. Mutant thalamic fibers form an aberrant bundle (arrows in **f**,**h**). (**i**,**j**) Sections in the normal (**i**) and mutant (**j**) cortex at P0. Note the radial bundles (arrowheads in **j**, left) and the abnormal subpial fascicles (arrow in **j**, right) in the mutant. (**k**,**l**) Sections in normal (**k**) and mutant (**l**) midbrain. The medial lemniscus (arrow in **k**) and the corticospinal tract (arrowhead in **k**) are poorly defined in the mutant. (**m**,**n**) Views of normal (**m**) and mutant (**n**) hindbrain. The spinocerebellar tract (arrowhead in **n**), the pyramidal tract (arrowhead in **m**) and other unidentified longitudinal fascicles (asterisk in **n**) are abnormal in the mutant. CX, cortex; GE, ganglionic eminence; STR, striatum; TE, tectum; TEG, tegmentum; TH, thalamus; ac, anterior commissure; cc, corpus callosum; fr, fasciculus retroflexus; int, internal capsule; ml, medial lemniscus; mtt, mammillothalamic tract; IZ, intermediate zone; PIA, pial surface. (**o**,**p**) Electron micrographs of a normal neuropil (**o**) and dilated axonal profiles (asterisks in **p**) in mutant cortical marginal zone at P0. PIA, pial surface; EF, glial endfeet. Bars, 5 μm.

absence of internal capsule, the shape of the thalamus was modified, making it difficult to study all thalamic components.

Neurofilament staining at E14.5 (**Fig. 3a–d**) and P0 (**Fig. 3e–n**) confirmed the absence of anterior commissure and internal capsule in the mutant brain (**Fig. 3a**,**b** and **3e–h**) and showed a reduction of fibers in the cortical intermediate zone and abnormal small radial fascicles in the upper cortical tier (**Fig. 3i**,**j**). A large aberrant tract originated from the mutant thalamus, but instead of making a sharp turn toward the internal capsule like its normal counterpart, it descended laterally to the hypothalamic region and turned around the basal forebrain to cross the tissue and enter the cortical marginal zone (**Fig. 3e–h**). When examined by electron microscopy, the newborn mutant and normal cortices contained similar resident neurons and neuropil (**Fig. 3o**). We observed swollen, moderately osmiophilic processes in the mutant but not in the normal cortical marginal zone (**Fig. 3p**). They were evocative of axonal swellings or spheroids, suggesting that some derailed axons might undergo degeneration.

We also detected anomalies of longitudinal tracts in more caudal regions. The corticospinal tract was diminutive, and we could not identify the medial lemniscus (**Fig. 3k**,**l**). The posterior spinocerebellar tract appeared dissociated, and many longitudinal fiber bundles in the mutant hindbrain tegmentum and dorsal spinal cord were reduced in size, poorly fasciculated or both (**Fig. 3c**,**d** and **3m**,**n**). Presumably, such anomalies could contribute to defective ventilation and neonatal

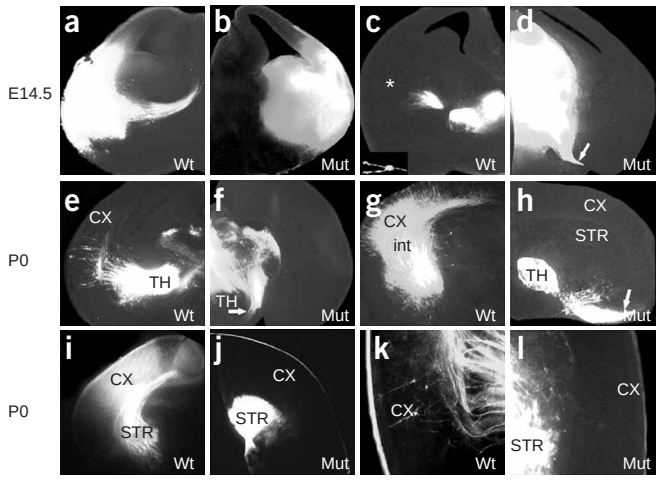


**Figure 4** Axon tracing shows abnormal development of thalamocortical and corticofugal projections. (**a**–**d**) Fiber tracing at E14.5, by DiI placement in the cortex (**a**,**b**) or thalamus (**c**,**d**) in normal (Wt, **a**,**c**) and mutant (Mut, **b**,**d**) brains. The asterisk and inset in **c** show a cell labeled in the ganglionic eminence. The arrow in **d** illustrates the abnormal thalamofugal bundle. (**e**–**h**) Fiber tracing at P0 by DiI placement in the thalamus of normal (**e**,**g**) and mutant brains (**f**,**h**). Arrows in **f** and **h** show the abnormal thalamic bundle that enters the mutant basal forebrain. (**i**–**l**) DiI crystal placement in the normal (**i**,**k**) and mutant striatum (**j**,**l**). Labeling of cortical neurons is seen in the normal but not in the mutant brain. CX, cortex; STR, striatum; TH, thalamus; int, internal capsule.

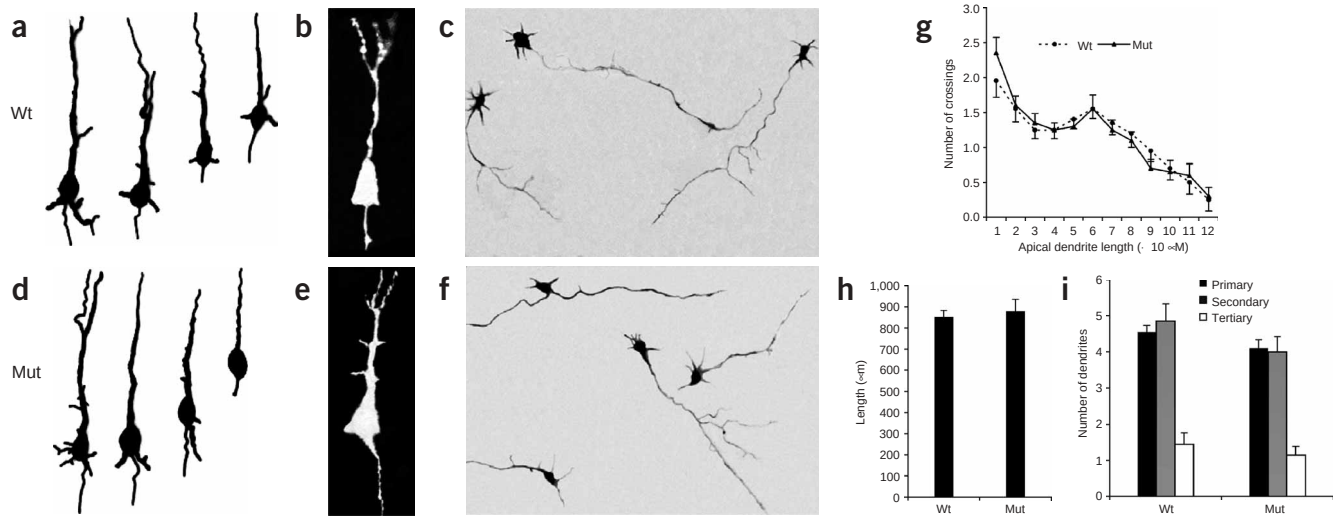


**Figure 5** *Celsr3* inactivation does not alter dendritic development. (**a**–**f**) Examples of normal (Wt, **a**–**c**) and mutant (Mut, **d**–**f**) cortical neurons at P0 (**a**,**d** stained with the Golgi method; **b**,**e** after DiI labeling) and in primary culture at E16.5 (**c**,**f** stained with an anti-Map2 antibody). (**g**) Sholl analysis[21] of Golgi-impregnated neurons ($n = 20$ of each genotype). (**h**,**i**) Studies of dendritic length (**h**) and branching pattern (primary, secondary and tertiary, **i**) in cultured neurons[22]. $n = 20$ of each genotype. Error bars, s.e.m.



lethality. By contrast, several tracts, including the fasciculus retroflexus, the mammillothalamic tract (**Fig. 3k**,**l**), the optic chiasm, optic tract, the olfactory tract and the intraparenchymal path of cranial nerves, were unaffected by the mutation.

We studied the pattern of developing connections by DiI tracing. At E14.5, crystal placement in the normal cortex resulted in filling of corticofugal fibers directed toward the thalamus (**Fig. 4a**), whereas in mutant animals, it stained large bundles that ran toward but did not traverse the ganglionic eminence (**Fig. 4b**). Dye placement in the normal thalamus labeled thalamocortical fibers capped with growth cones that entered the internal capsule but did not reach the cortex (**Fig. 4c**). A few cells were labeled in the ganglionic eminence (**Fig. 4c**, inset), as has been described by others[18]. In mutant brains, fibers labeled after thalamic dye placement ran ventrally in the diencephalon toward the basal forebrain (**Fig. 4d**). At P0, dye placement in the thalamus (**Fig. 4e**–**h**) resulted in a profuse labeling of the internal capsule and cortical neurons in normal brains, whereas in mutant brains, cortical neurons were not labeled, but there were large fluorescent bundles in the homolateral cortical marginal zone. Crystal placement in the striatum (**Fig. 4i**–**l**) resulted in strong labeling of the normal internal capsule and cortical neurons but did not stain any structure in the mutant. DiI injections in the cortex resulted in prominent labeling in the thalamus of normal but not mutant animals, except in the cortex adjacent to the injection site.

### *Celsr3* inactivation does not alter neuronal maturation

In flies, in addition to being involved in the development of longitudinal axonal tracts, *fmi* is also implicated in dendrite development[19]. Furthermore, inactivation of rodent *Celsr2* by RNA interference *in vitro* interferes with dendrite development[20]. Although dendritic maturation is rudimentary at P0 and happens mostly postnatally, we studied arborizations of cortical neurons by Golgi impregnation and DiI labeling, and we examined dendrites in primary cultures of E16.5 cortical neurons that were allowed to develop *in vitro* for 6 d (**Fig. 5a**–**f**). At P0, the mean lengths of apical dendrites were similar in normal (104 ± 4 μm, s.e.m.) and mutant (99 ± 4 μm) animals (*t*-test, $P = 0.33$). The ramifications of dendritic trees, measured using the Sholl method[21] and analyzed with the Kruskal-Wallis test, were comparable in both genotypes (**Fig. 5g**). In cultured neurons (**Fig. 5c**,**f**), the length and number of dendritic branches (stained with an antibody to Map2 and analyzed as

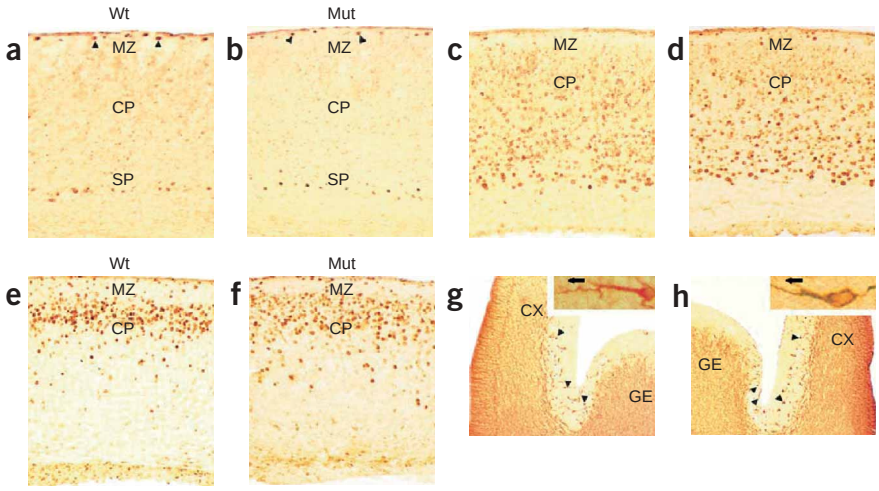


**Figure 6** Normal cortical maturation in *Celsr3* mutant mice. (**a**–**f**) Frontal sections at P0 stained with an anti-BrdU antibody after tracer administration at E10.5 (**a**,**b**), E12.5 (**c**,**d**) and E14.5 (**e**,**f**). No difference in the distribution of labeled cells is seen between normal (Wt, **a**,**c**,**e**) and mutant mice (Mut, **b**,**d**,**f**). MZ, marginal zone; CP, cortical plate; SP, subplate. (**g**,**h**) E14.5 brain sections stained with an anti-Map2 antibody to detect tangentially migrating neurons (arrowheads) in wild-type (**g**) and in *Celsr3* mutant mice (**h**). Insets show example of labeled neurons; arrows indicate the direction of the cortex. CX, cortex; GE, ganglionic eminence.

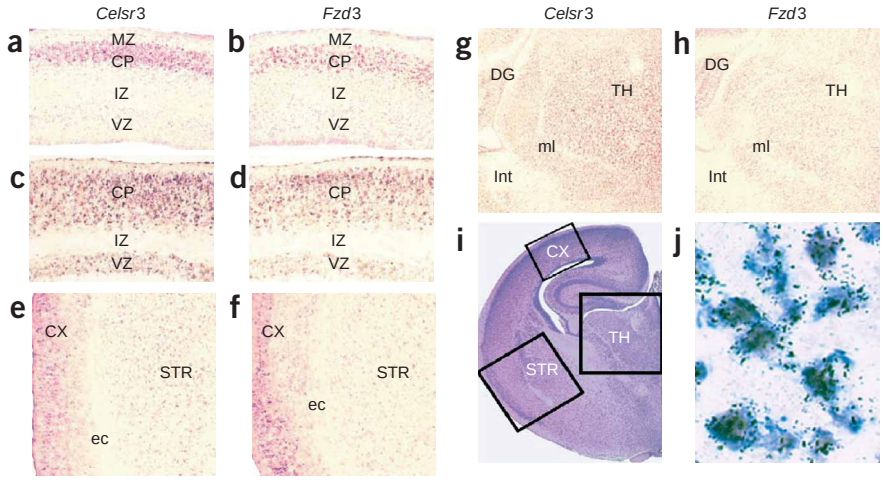


**Figure 7** *Celsr3* and *Fzd3* coexpression. (**a**–**h**) *In situ* hybridization with digoxigenin-labeled riboprobes showing *Celsr3* and *Fzd3* mRNA expression in the E14.5 cortex (**a**,**b**) and in the forebrain at P0 (**c**–**h**). The locations of the fields illustrated in (**c**–**h**) are outlined in panel (**i**). Note the similarity of both patterns, with high expression in the cortical plate at E14.5. MZ, marginal zone; CP, cortical plate; IZ, intermediate zone; VZ, ventricular zone; STR, striatum; TH, thalamus; DG, dentate gyrus; CX, cortex; ec, external capsule; int, internal capsule; ml, medial lemniscus. (**j**) High-magnification photomicrograph showing expression of *Celsr3* (digoxigenin probe, blue) and *Fzd3* (radioactive probe, black dots) mRNA in cortical neurons.

described[22]) were not statistically different (**Fig. 5h**,**i**). These results showed that *Celsr3* did not regulate prenatal dendritic growth.

To study cortical maturation, we labeled cohorts of normal and *Celsr3* mutant cortical neurons by bromodeoxyuridine (BrdU) injections at E10.5, E12.5 and E14.5 and examined the distribution of labeled neurons at P0. After we labeled preplate neurons at E10.5, we detected two contingents of cells in the marginal zone and subcortex, showing that preplate splitting occurred normally in *Celsr3* mutant mice (**Fig. 6a**,**b**). In both genotypes, neurons labeled by injection of BrdU at E12.5 and E14.5 migrated toward the inner and outer tier, respectively, of the cortical ribbon, indicating that the normal inside-to-outside gradient of cortical maturation is not affected by mutation of the *Celsr3* gene (**Fig. 6c–f**). In contrast to the marked alterations of thalamocortical axonal tracts, tangential neuronal migration from the ganglionic eminence, studied using anti-Map2 immunohistochemistry[23], occurred normally in *Celsr3* mutant mice (**Fig. 6g**,**h**).

### *Celsr3* and *Fzd3* are expressed together in developing neurons

As *Celsr3* and *Fzd3* mutant mice have similar CNS malformations (see Discussion), we examined the expression of corresponding mRNA using *in situ* hybridization at E14.5 and P0. At E14.5, *Celsr3* and *Fzd3* probes were detected at high levels in postmigratory neurons in the cortical plate and at lower concentrations in the ventricular and intermediate zones (**Fig. 7a**,**b**). At P0, the distribution of both signals was more widespread. Although expression remained the highest in the cortical ribbon, it was moderate in the ventricular zone (**Fig. 7c**,**d**). Both genes were expressed in the striatum and thalamus, although the *Celsr3* signal was stronger in the latter (**Fig. 7e–i**). Double *in situ* hybridization with $^{33}$P-labeled *Fzd3* and digoxigenin-labeled *Celsr3* riboprobes confirmed that both genes were expressed in the same cells (**Fig. 7j**). We also compared *Celsr3* expression at P0 to that of the PCP gene orthologs *Dvl1–Dvl3*, *Vangl1*, *Vangl2*, *Prickle1* and *Prickle2*. All showed overlapping expression patterns, suggesting that they are expressed in *Celsr3*-positive cells (data not shown).

## DISCUSSION

Our data indicate that *Celsr3* is necessary for the development of the anterior commissure; the corticosubcortical, thalamocortical and corticospinal tracts; the medial lemniscus; and the spinocerebellar tract and several longitudinal bundles in the hindbrain and spinal cord, but not for the development of other tracts, development of the peripheral nervous system or architectonic organization.

### *Celsr* genes and brain development

As mentioned above, in flies, *fmi*, frizzled (*fz*), dishevelled (*dsh*), van gogh (*vang*) and prickle (*pk*) form a family of 'core PCP genes'[24,25]. *Fmi* null mutations are embryonically lethal[4] because of defective axonal fiber tracts in the CNS[3], which is evocative of the phenotype in *Celsr3* mutant mice. Hypomorphic alleles are viable in the homozygote condition but still show anomalies in PCP[4]. Similarly, defective PCP is seen when embryonic lethality is corrected by CNS-specific gene rescue[3]. This suggests that the regulation of tract formation and PCP are mediated by separate functions of the flamingo protein. Both embryonic lethality and the defect in PCP are *fz* dependent but independent of wingless (*wg*). *Fmi* is also involved in the development of dendritic fields, independently of *fz*[19]. Thus, in the fly, *fmi* regulates three largely independent events: axonal tract formation, PCP and dendrite development.

In mice, whereas *Celsr3* is involved in the formation of fiber tracts, published evidence suggests that *Celsr1* and *Celsr2* regulate PCP in the neural plate and dendrite deployment, respectively. *Celsr1* gene expression is confined to the neuroepithelium[6–8], and two different point mutations generate anomalies of the polarity of inner ear hair cells and defective neural tube closure, respectively, in heterozygous and homozygous mice, indicating a key role in PCP[12]. In contrast, *Celsr3* mRNA is not expressed in the developing ear, and *Celsr3*-deficient mice do not have any anomaly of neural tube closure that would indicate a defect in PCP in the strict sense. *Celsr2* is widely expressed in neuronal precursors and postmigratory cells during development and in the adult[8]. Inactivation of *Celsr2* using RNA interference in postnatal brain slices alters dendrite development; whether this effect is dependent on frizzled has not been investigated[20]. This suggests that *Celsr2* regulates development and maintenance of dendritic fields, which are subject to plastic changes throughout life. In *Celsr3* mutant mice, nerve cell impregnations and studies of cortical neurons in primary culture did not show any anomalies in dendrites. As dendritic development proceeds mostly after birth, and *Celsr3* mutant mice died at P0, an influence of *Celsr3* on dendritic maturation could not be excluded; it may manifest itself at later developmental stages. This question could be addressed using *in vitro* RNA interference in postnatal brain slices[20] or by studying the maturation in mutant neurons in chimeric or viable conditional *Celsr3* mutant mice. Altogether, evidence available thus far suggests that the three functions attributed to *fmi* in the regulation of PCP, dendritic fields and axonal tracts may be fulfilled by the three ortholog genes *Celsr1–Celsr3* in mammals.

### *Celsr3* and *Fzd3* mutant mice have similar phenotypes

The control of axonal growth and guidance is highly complex[26]. Gene targeting in mice has identified transcription factors, secreted molecules and cell surface molecules with different roles in this process. As discussed in more detail below in the context of thalamocortical development, *Celsr3* mutant mice share only limited features with other mutants, with the exception of frizzled-3- (*Fzd3*) null mice[16,27]. Like *Celsr3* mutants, *Fzd3*-null mice die shortly after birth, probably of central ventilation failure, with no defect in lung or respiratory muscles. In both mutant mice, the internal capsule, anterior commissure and many longitudinal axonal bundles are absent, whereas the hippocampal system, fasciculus retroflexus and several other axonal pathways are normal. Both have cortical hypoplasia, ventricular dilatation and a protruding globular striatum. Moreover, the timing of neurogenesis and neurite development *in vivo* and *in vitro* were unaffected. Histological examination of an *Fzd3* mutant E18 brain (provided by Y. Wang and J. Nathans, Johns Hopkins University School of Medicine, Baltimore, Maryland, USA) confirmed that the two malformations are indistinguishable. *Fzd3* null mice have a more severe phenotype than *Celsr3* mutant mice, including death soon after birth, a curled tail, posterior limb deformity and occasional cranioschisis[16]. This could be due to different genetic backgrounds or it could reflect a *Celsr3*-independent role of *Fzd3* in neural tube closure, possibly in interaction with *Celsr1*. The expression of *Celsr3* and *Fzd3* mRNA in the same cells and the similarity of the mutant phenotypes strongly suggested that both genes participate in a common genetic pathway in mammals, as their orthologs do in flies. It is tempting to speculate that mammalian orthologs of other core PCP genes (dishevelled, prickle-like and van gogh–like) could also be involved.

### *Celsr3* and thalamocortical development

In *Celsr3* mutant mice, the neocortex is almost entirely disconnected from subcortical structures, mimicking a 'cortex isolé' *in vivo*. No thalamic axon reaches the cortex by the normal route, and no corticofugal axon extends beyond the external capsule. Thalamic fibers depart at the normal time toward the hemispheres, but instead of turning in the internal capsule, they travel ventrally in the diencephalon and then turn externally through the basal forebrain toward the cortical marginal zone. As in the normal cortex, axons of mutant cortical neurons emanate from the basal soma and course radially toward the subcortex, where they run tangentially. However, they could not be traced beyond the external capsule.

The mechanisms that regulate the patterning of thalamocortical connections are not fully understood[28]. In the absence of cortical fibers, thalamic axons cannot find their way to the cortex and, reciprocally, cortical axons are guided in their descent by thalamic fibers[28–31], suggesting that thalamocortical and corticothalamic fibers interact synergistically in the internal capsule. Developing thalamocortical and corticothalamic axons need to cross two critical boundaries, the diencephalon-telencephalon junction (DTJ) and the pallial/subpallial boundary (PSPB). In addition to their reciprocal interaction mentioned above, it is generally believed that specific guidance cues are provided by guidepost cells at the DTJ, PSPB and along the pathway[28].

Gene inactivation experiments in mice have identified many genes implicated in the development of thalamocortical connections[28]. The growing list includes many encoding transcription factors, such as *Pax6* (refs. 32–34), *Emx1* and *Emx2* (refs. 35,36), *Gbx2* (ref. 31), *Ebf1* (ref. 37), *Dlx1* and *Dlx2* (refs. 37,38), as well as *Tbr1* (ref. 39), *Nr2f1* (also known as *COUP-TF1*) (ref. 40) and *Ascl1* (also known as *Mash1*; refs. 41,42). These genes are expressed in the thalamus, basal forebrain, cortical preplate or combinations thereof. Transcription factors may act intrinsically on the formation of axons or indirectly by altering the fate of guidepost cells that are located along the path and responsible for dispensing guidance cues. A second set of genes implicated in thalamocortical development encode secreted or surface molecules such as Slit1 and Slit2 (ref. 43), netrin[44] and its receptors Unc5c and Dcc[45], as well as some semaphorins, particularly semaphorin 6A (ref. 46). Among the mutant mice with alterations of thalamocortical development, the anomalies described in *Ascl1* mutants[41,42] are reminiscent of those in *Celsr3*- and *Fzd3*-deficient mice, hinting at possible interactions that should be investigated further.

In sum, our results demonstrate a critical role for the protocadherin Celsr3 in axonal development. *Celsr3* and *Fzd3* are the first identified members of a genetic pathway that bears marked analogy with the pathways that control PCP in Drosophila and neural tube closure in vertebrates. The fact that other major fiber tracts are not affected by inactivation of *Celsr3* or *Fzd3* indicates that other, complementary systems remain to be identified.

## METHODS

**Gene targeting.** The procedure for generating *Celsr3* mutant mice is described in detail in the **Supplementary Note**, **Supplementary Figure 1** and **Supplementary Table 1**. All animal procedures were performed under guidelines of institutional animal ethics committees of the University of Louvain.

**Histology and immunohistochemistry.** For routine histological examination, fixation was performed with 4% paraformaldehyde (PFA) in PBS or with Bouin's fluid followed by embedding in paraplast. Sections were cut at 8 μm and stained with hematoxylin-eosin. For immunohistochemistry with antibodies against neurofilaments, Map2 and BrdU, paraffin sections were incubated, respectively, with monoclonal antibody 2H3 (Hybridoma Bank, 1:500), anti-Map2 (Sigma M4403) or anti-BrdU (Becton Dickinson). Visualization was carried out with a Duet Kit (Dako Cytomation).

**Golgi impregnation.** Golgi staining of newborn brains was done using the rapid Golgi and Rethelyi protocols[47]. Blocks were embedded in 4% agarose, cut serially at 150 μm thickness with a vibratome, dehydrated and mounted with Neomount (VWR). Drawings were made with a camera lucida. Dendritic arbors were analyzed with the Sholl method, using the Kruskal-Wallis test at a significance level of 0.05 (ref. 21).

**DiI tracing.** DiI crystals (D3911, Molecular Probes) were implanted in target areas of PFA-fixed brains using tungsten needles. Blocks were incubated in the dark at 37 °C in PBS containing 0.01% sodium azide for 2–4 weeks. They were then embedded in 4% agarose for preparation of 150-μm-thick vibratome sections that were mounted with Vectashield (Vector Lab) and examined under epifluorescence microscopy with a rhodamine filter.

**Whole-mount staining of diaphragms.** Studies of the innervation of the diaphragm were carried out using immunohistochemical staining of whole-mount preparations with polyclonal antibody NF-150 (Chemicon, 1:400) directed against neurofilaments, as described[48]. This antibody is known to stain fine nerve terminals and gave the best signal-to-noise ratio.

**Electron microscopy.** Newborn normal and mutant brains were fixed by perfusion of 2% glutaraldehyde, 2% PFA in phosphate buffer (0.1 M, pH 7.5) and postfixed overnight in the same fixative. Blocks were postfixed with osmium and thin sections were prepared and stained with uranyl acetate and lead citrate using standard protocols.

***In situ* hybridization.** Total RNA was extracted from normal and *Celsr3* mutant newborn mouse brains using an RNeasy kit (Qiagen) according to the manufacturer's instructions. First-strand cDNA was synthesized from 2 μg of total RNA using Superscript III reverse transcriptase (Invitrogen). cDNA sequences corresponding to parts of the *Celsr3*, *Vangl1*, *Vangl2*, *Prickle1*, *Prickle2*, *Dvl1–Dvl3* and *Fzd3* genes were amplified by RT-PCR using the oligonucleotide primers described in **Supplementary Table 2**. Procedures for simple and double *in situ* hybridization with radiolabeled and digoxigenin-labeled probes have been described previously[49].

**Primary neuronal cultures.** E16.5 embryonic cortices were dissected in ice-cold $Ca^{2+}$ and $Mg^{2+}$ free Hanks' balanced salt solution (CMF-HBSS) and dissociated with 0.1% trypsin (Invitrogen) followed by DNase I (Invitrogen). Cells were plated on poly-L-lysine–coated glass coverslips and cultured in DMEM-F12 supplemented with B27 (Invitrogen) as described[50]. After 6 d in culture, neurons were fixed in PFA and labeled by immunocytochemistry with anti-Map2 to stain dendrites. Dendritic ramifications were analyzed as described[22], using *t*-tests at a *P*-level of 0.05.

**Study of cortical neurogenesis.** Pregnant mothers were injected intraperitoneally with BrdU (20 mg $kg^{-1}$). Newborn mice were anesthetized on ice, and brains were fixed in paraformaldehyde (4% in PBS). Paraffin sections were stained with an anti-BrdU antibody (Becton Dickinson).

*Note: Supplementary information is available on the Nature Neuroscience website.*

**ACKNOWLEDGMENTS**

We thank O. De-Backer for his support and help with embryonic stem cells, C. Lambert de Rouvroit for discussion, and V. Bonte, I. Lambermont and E. Paître for technical assistance. We also wish to thank J. Nathans and Y. Wang for discussion and for generously providing the *Fzd3* mutant sample, as well as A. Stoykova and A. Mallamaci for *Pax6* and *Emx* mutant samples. This work was supported by grants FRFC 2.4504.01, FRSM 3.4529.03, LN 2.4504.01, by the Fondation Médicale Reine Elisabeth, all from Belgium, and by grant QLG3-CT-2000-00158 from the European Union.

**COMPETING INTERESTS STATEMENT**

The authors declare that they have no competing financial interests.

Received 8 February; accepted 1 March 2005
Published online at http://www.nature.com/natureneuroscience/



1. Nakayama, M. *et al.* Identification of high-molecular-weight proteins with multiple EGF-like motifs by motif-trap screening. *Genomics* **51**, 27–34 (1998).
2. Hadjantonakis, A.K. *et al.* Celsr1, a neural-specific gene encoding an unusual seven-pass transmembrane receptor, maps to mouse chromosome 15 and human chromosome 22qter. *Genomics* **45**, 97–104 (1997).
3. Usui, T. *et al.* Flamingo, a seven-pass transmembrane cadherin, regulates planar cell polarity under the control of Frizzled. *Cell* **98**, 585–595 (1999).
4. Chae, J. *et al.* The *Drosophila* tissue polarity gene starry night encodes a member of the protocadherin family. *Development* **126**, 5421–5429 (1999).
5. Hadjantonakis, A.K., Formstone, C.J. & Little, P.F. mCelsr1 is an evolutionarily conserved seven-pass transmembrane receptor and is expressed during mouse embryonic development. *Mech. Dev.* **78**, 91–95 (1998).
6. Formstone, C.J. & Little, P.F. The flamingo-related mouse Celsr family (Celsr1–3) genes exhibit distinct patterns of expression during embryonic development. *Mech. Dev.* **109**, 91–94 (2001).
7. Shima, Y. *et al.* Differential expression of the seven-pass transmembrane cadherin genes Celsr1–3 and distribution of the Celsr2 protein during mouse development. *Dev. Dyn.* **223**, 321–332 (2002).
8. Tissir, F., De-Backer, O., Goffinet, A.M. & Lambert de Rouvroit, C. Developmental expression profiles of Celsr (Flamingo) genes in the mouse. *Mech. Dev.* **112**, 157–160 (2002).
9. Lu, B., Usui, T., Uemura, T., Jan, L. & Jan, Y.N. Flamingo controls the planar polarity of sensory bristles and asymmetric division of sensory organ precursors in *Drosophila*. *Curr. Biol.* **9**, 1247–1250 (1999).
10. Senti, K.A. *et al.* Flamingo regulates R8 axon-axon and axon-target interactions in the *Drosophila* visual system. *Curr. Biol.* **13**, 828–832 (2003).
11. Lee, R.C. *et al.* The protocadherin Flamingo is required for axon target selection in the *Drosophila* visual system. *Nat. Neurosci.* **6**, 557–563 (2003).
12. Curtin, J.A. *et al.* Mutation of Celsr1 disrupts planar polarity of inner ear hair cells and causes severe neural tube defects in the mouse. *Curr. Biol.* **13**, 1129–1133 (2003).
13. Kibar, Z. *et al.* Ltap, a mammalian homolog of *Drosophila* Strabismus/Van Gogh, is altered in the mouse neural tube mutant Loop-tail. *Nat. Genet.* **28**, 251–255 (2001).
14. Murdoch, J.N., Doudney, K., Paternotte, C., Copp, A.J. & Stanier, P. Severe neural tube defects in the loop-tail mouse result from mutation of Lpp1, a novel gene involved in floor plate specification. *Hum. Mol. Genet.* **10**, 2593–2601 (2001).
15. Hamblet, N.S. *et al.* Dishevelled 2 is essential for cardiac outflow tract development, somite segmentation and neural tube closure. *Development* **129**, 5827–5838 (2002).
16. Wang, Y., Thekdi, N., Smallwood, P.M., Macke, J.P. & Nathans, J. Frizzled-3 is required for the development of major fiber tracts in the rostral CNS. *J. Neurosci.* **22**, 8563–8573 (2002).
17. Volynski, K.E. *et al.* Latrophilin fragments behave as independent proteins that associate and signal on binding of LTX(N4C). *EMBO J.* **23**, 4423–4433 (2004).
18. Metin, C. & Godement, P. The ganglionic eminence may be an intermediate target for corticofugal and thalamocortical axons. *J. Neurosci.* **16**, 3219–3235 (1996).
19. Gao, F.B., Kohwi, M., Brenman, J.E., Jan, L.Y. & Jan, Y.N. Control of dendritic field formation in *Drosophila*: the roles of flamingo and competition between homologous neurons. *Neuron* **28**, 91–101 (2000).
20. Shima, Y., Kengaku, M., Hirano, T., Takeichi, M. & Uemura, T. Regulation of dendritic maintenance and growth by a mammalian 7-pass transmembrane cadherin. *Dev. Cell* **7**, 205–216 (2004).
21. Sholl, D.A. Dendritic organization in the neurons of the visual and motor cortices of the cat. *J. Anat.* **87**, 387–406 (1953).
22. Rosso, S.B., Sussman, D., Wynshaw-Boris, A. & Salinas, P.C. Wnt signaling through Dishevelled, Rac and JNK regulates dendritic development. *Nat. Neurosci.* **8**, 34–42 (2005).
23. Tamamaki, N., Fujimori, K.E. & Takauji, R. Origin and route of tangentially migrating neurons in the developing neocortical intermediate zone. *J. Neurosci.* **17**, 8313–8323 (1997).
24. Adler, P.N. & Lee, H. Frizzled signaling and cell-cell interactions in planar polarity. *Curr. Opin. Cell Biol.* **13**, 635–640 (2001).
25. Uemura, T. & Shimada, Y. Breaking cellular symmetry along planar axes in *Drosophila* and vertebrates. *J. Biochem.* **134**, 625–630 (2003).
26. Guan, K.L. & Rao, Y. Signalling mechanisms mediating neuronal responses to guidance cues. *Nat. Rev. Neurosci.* **4**, 941–956 (2003).
27. Lyuksyutova, A.I. *et al.* Anterior-posterior guidance of commissural axons by Wnt-frizzled signaling. *Science* **302**, 1984–1988 (2003).
28. Lopez-Bendito, G. & Molnar, Z. Thalamocortical development: how are we going to get there? *Nat. Rev. Neurosci.* **4**, 276–289 (2003).
29. Molnar, Z. & Blakemore, C. Lack of regional specificity for connections formed between thalamus and cortex in coculture. *Nature* **351**, 475–477 (1991).
30. Molnar, Z., Higashi, S. & Lopez-Bendito, G. Choreography of early thalamocortical development. *Cereb. Cortex* **13**, 661–669 (2003).
31. Miyashita-Lin, E.M., Hevner, R., Wassarman, K.M., Martinez, S. & Rubenstein, J.L. Early neocortical regionalization in the absence of thalamic innervation. *Science* **285**, 906–909 (1999).
32. Stoykova, A., Treichel, D., Hallonet, M. & Gruss, P. Pax6 modulates the dorsoventral patterning of the mammalian telencephalon. *J. Neurosci.* **20**, 8042–8050 (2000).
33. Pratt, T. *et al.* Disruption of early events in thalamocortical tract formation in mice lacking the transcription factors Pax6 or Foxg1. *J. Neurosci.* **22**, 8523–8531 (2002).
34. Jones, L., Lopez-Bendito, G., Gruss, P., Stoykova, A. & Molnar, Z. Pax6 is required for the normal development of the forebrain axonal connections. *Development* **129**, 5041–5052 (2002).
35. Mallamaci, A., Muzio, L., Chan, C.H., Parnavelas, J. & Boncinelli, E. Area identity shifts in the early cerebral cortex of Emx2−/− mutant mice. *Nat. Neurosci.* **3**, 679–686 (2000).
36. Yoshida, M. *et al.* Emx1 and Emx2 functions in development of dorsal telencephalon. *Development* **124**, 101–111 (1997).
37. Garel, S., Yun, K., Grosschedl, R. & Rubenstein, J.L. The early topography of thalamocortical projections is shifted in Ebf1 and Dlx1/2 mutant mice. *Development* **129**, 5621–5634 (2002).
38. Anderson, S.A. *et al.* Mutations of the homeobox genes Dlx-1 and Dlx-2 disrupt the striatal subventricular zone and differentiation of late born striatal neurons. *Neuron* **19**, 27–37 (1997).
39. Hevner, R.F., Miyashita-Lin, E. & Rubenstein, J.L. Cortical and thalamic axon pathfinding defects in Tbr1, Gbx2, and Pax6 mutant mice: evidence that cortical and thalamic axons interact and guide each other. *J. Comp. Neurol.* **447**, 8–17 (2002).
40. Zhou, C. *et al.* The nuclear orphan receptor COUP-TFI is required for differentiation of subplate neurons and guidance of thalamocortical axons. *Neuron* **24**, 847–859 (1999).
41. Tuttle, R., Nakagawa, Y., Johnson, J.E. & O'Leary, D.D. Defects in thalamocortical axon pathfinding correlate with altered cell domains in Mash-1-deficient mice. *Development* **126**, 1903–1916 (1999).
42. Schuurmans, C. & Guillemot, F. Molecular mechanisms underlying cell fate specification in the developing telencephalon. *Curr. Opin. Neurobiol.* **12**, 26–34 (2002).
43. Bagri, A. *et al.* Slit proteins prevent midline crossing and determine the dorsoventral position of major axonal pathways in the mammalian forebrain. *Neuron* **33**, 233–248 (2002).
44. Metin, C., Deleglise, D., Serafini, T., Kennedy, T.E. & Tessier-Lavigne, M. A role for netrin-1 in the guidance of cortical efferents. *Development* **124**, 5063–5074 (1997).
45. Finger, J.H. *et al.* The netrin 1 receptors Unc5h3 and Dcc are necessary at multiple choice points for the guidance of corticospinal tract axons. *J. Neurosci.* **22**, 10346–10356 (2002).
46. Leighton, P.A. *et al.* Defining brain wiring patterns and mechanisms through gene trapping in mice. *Nature* **410**, 174–179 (2001).
47. Rethelyi, M. Cell and neuropil architecture of the intermedio-lateral (sympathetic) nucleus of cat spinal cord. *Brain Res.* **46**, 203–213 (1972).
48. Lin, W. *et al.* Aberrant development of motor axons and neuromuscular synapses in erbB2-deficient mice. *Proc. Natl. Acad. Sci. USA* **97**, 1299–1304 (2000).
49. Tissir, F., Wang, C.E. & Goffinet, A.M. Expression of the chemokine receptor Cxcr4 mRNA during mouse brain development. *Brain Res. Dev. Brain Res.* **149**, 63–71 (2004).
50. Jossin, Y. *et al.* The central fragment of Reelin, generated by proteolytic processing *in vivo*, is critical to its function during cortical plate development. *J. Neurosci.* **24**, 514–521 (2004).